Smart Antenna Systems for Mobile Communications

ABSTRACT

Much more than a simple antenna array that provides tunable phase shifts, the smart antenna is an advanced multiple-antenna system for optimizing network infrastructure, costs, and performance to meet the growing requirements of future mobile broadband services. Smart antennas accomplished this by utilizing the full potential of radio resources in the spatial domain. This report presents two types of smart antennas, the system elements of an adaptive antenna, and various theories, benefits and drawbacks involved in smart antennas. In the end, a simulation and analysis is also included to examine the performance of a smart antenna.

1. INTRODUCTION

In recent years a substantial increase in the development of broadband wireless access technologies for evolving wireless Internet services and improved cellular systems has been observed. The rise in traffic has put a demand on both manufacturers and operators to provide sufficient capacity in the networks. Throughout the world, the entire wireless industry is seeking new solutions for utilizing radio resources more efficiently.

There have been a few proposals made to improve radio resource efficiency for the next generation mobile communication systems. One approach is to reduce cell size in the macro-spatial domain, whereby radio resources are re-used due to the geographic isolation of different cells' radio signals. To this effect, great interest has been shown in various small cell technologies, the most recent example being the deployment of heterogeneous networks. But while deploying a large number of small cells may enable gains in capacity, the result is a higher need for backhaul resources and a more complex networking of numerous low-power base stations (BS) [1].

None of the proposals that include improved air interface and modulation schemes, and deployment of smaller radio cells with combinations of different cell types in hierarchical architectures have fully exploited the multiplicity of spatial channels that arises because each mobile user occupies a unique spatial location. Spatial domain is truly one of the new frontiers to be explored. The deployment of smart antenna system has emerged as one of the leading technologies for achieving high efficiency networks that maximize capacity and improve quality and coverage. It has received much attention in the last few years because they can increase system capacity (very important in urban and densely populated areas) by dynamically tuning out interference while focusing on the intended user along with impressive advances in the field of digital signal processing. Thus, the spatial dimension can be

exploited as a hybrid multiple access technique complementing frequency-division multiple access (FDMA), time-division multiple access (TDMA) and code-division multiple access (CDMA). This approach is usually referred to as space-division multiple access (SDMA) and enables multiple users within the same radio cell to be accommodated on the same frequency and time slot, as shown below [1]:

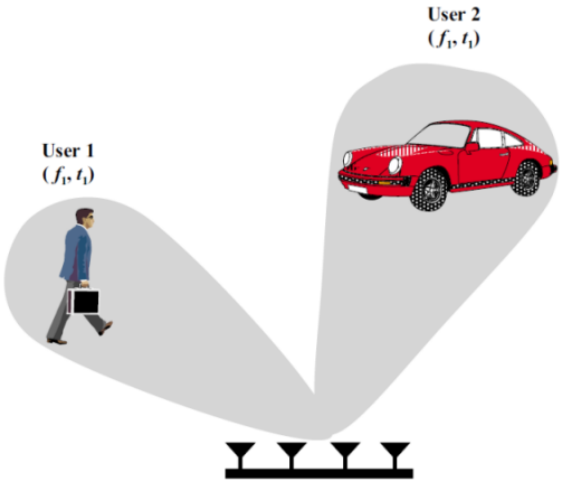

Figure 1: SDMA concept.

2. TYPES OF SMART ANTENNAS

Smart antenna systems can be categorized as either switched beam or adaptive antenna array systems [2]. The distinctions between the two major categories of smart antennas regarding the choices in transmit strategy are as follows:

- Switched Beam — a finite number of fixed, predefined patterns or combining strategies (sectors).
- Adaptive Array — an infinite number of patterns (scenario-based) that are adjusted in real time.

2.1 Switched Beam Antennas

Switched beam antennas are an extension of traditional cellular sectorization, which is usually composed of three 120° sectors [2]. The switched beam approach can further divide each sector into several sub-sectors as seen in Figure 2 below. The output from a switched beam is a grid of orthogonal beams, where each beam has a maximum toward some direction and minima toward the directions of all other beams. The best beam from the grid is selected based on an algorithm that optimizes the power or SINR. Due to the fixed pointing direction nature of the switched beam approach, it introduces cusping loss between beams, offers limited interference suppression, and is sensitive to false beam locking due to interference, shadowing, and wide angular spread.

The switched beam technique can be extended to achieve dynamic sectorization by optimizing sector coverage as a function of traffic requirements. Figure 3b gives an example where a narrower sector is

created from 60° to 120° by choosing the appropriate beams in order to support the increased traffic in the area (see Figure 3a), while the other two sectors have been widened accordingly. The result is to balance the load throughout the whole cell, hence improving the overall capacity. This technique gives reasonable benefits for non-uniform traffic scenarios (in practice, traffic during a day is highly time variant, e.g., high traffic demands in highways during morning-afternoon rush hours but lower during office hours and high traffic demands in office areas during office hours but low in the afternoon-night).

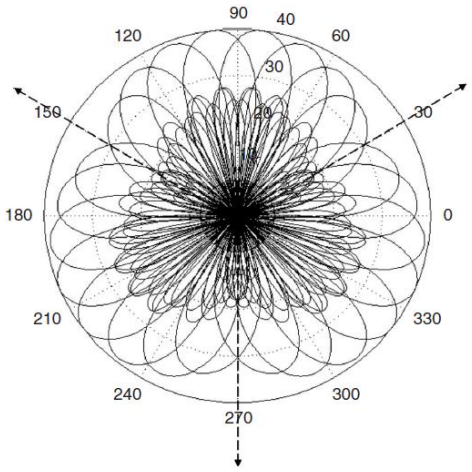

Figure 2: Switched beam antenna: grid of eight beams produced by a six-element linear array per sector.

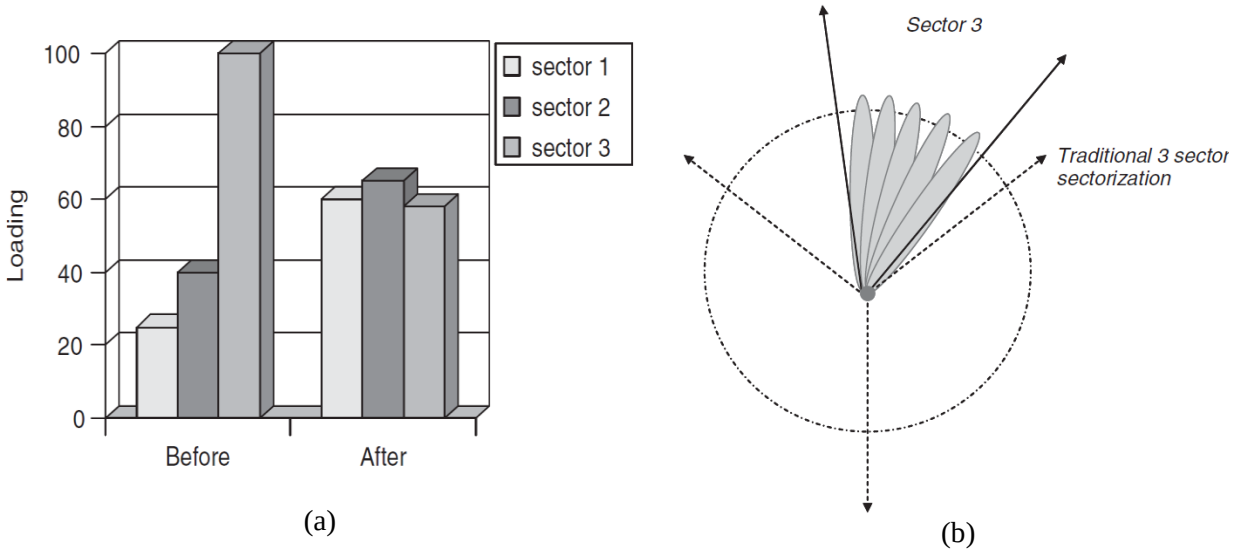

Figure 3: Dynamic sectorization: (a) loading before and after dynamic sectorization and (b) dynamic sectorization layout.

2.2 Adaptive Antenna Array s

Adaptive antenna array approach represents the most advanced beamforming technology to date [2]. Using a variety of novel signal-processing algorithms, the adaptive array takes advantage of its ability to distinguish between desired signals, multipath, and interfering signals as well as calculate their

directions of arrival. Adaptive arrays increase gain by continuously tracking the users with main lobes and interferers with nulls to ensure the link budget is constantly maximized.

Figure 4 illustrates different beam patterns of each smart antenna type in a scenario involving one desired signal and two co-channel interferers. Both antennas direct their main lobes in the direction of the signal of interest. The switched beam chooses the "best" beam from a grid of beams with fixed directions while the adaptive array chooses a more accurate placement for both main lobe and nulls, hence providing greater signal enhancement.

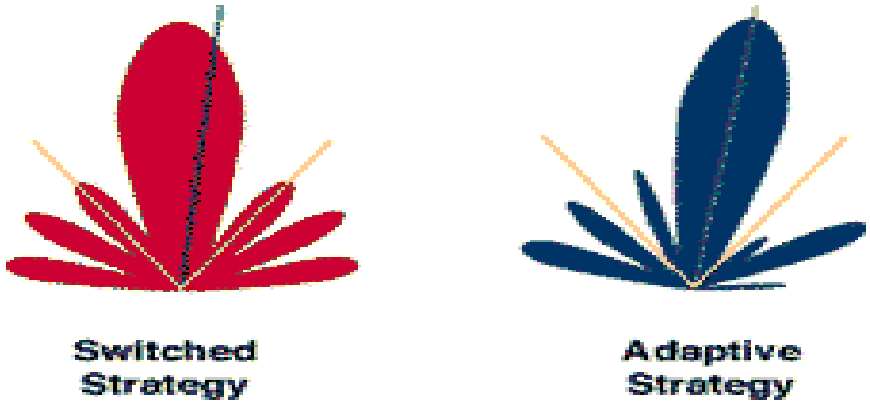

Figure 4: Smart antenna: switched beam versus adaptive array.

3. SYSTEM ELEMENTS OF A SMART ANTENNA

The adaptive antenna consists of the sensor array, the patternforming network, and the adaptive processor [3]:

i. *Sensor Array*: The sensor array consists of N sensors designed to receive (and transmit) signals. The physical arrangement of the array (linear, circular, cylindrical and two-dimensional etc.) can be chosen arbitrarily, depending on the required specifications. However, it places fundamental limitations on the capability of the adaptive antenna.

ii. *Patternforming Network*: The output of each of the N sensor elements is fed into the patternforming network, where the outputs are processed by linear time-variant (LTV) filters. These filters determine the directional pattern of the adaptive antenna. The outputs of the LTV filters are then summed to form the overall output $y(t)$. The complex weights of the LTV filters are determined by the adaptive processor.

iii. *Adaptive Processor*: The adaptive processor determines the complex weights of the patternforming network. The signals and known system properties used to compute the weights include the following:

- The signals received by the sensor array, i.e., $x_n(t)$, $n = 1, 2, \ldots, N$.
- The output of the adaptive antenna, i.e., $y(t)$.
- The *spatial structure* of the sensor array.

- The *temporal structure* of the received signal.
- Feedback signals from the mobiles.
- Network topology.

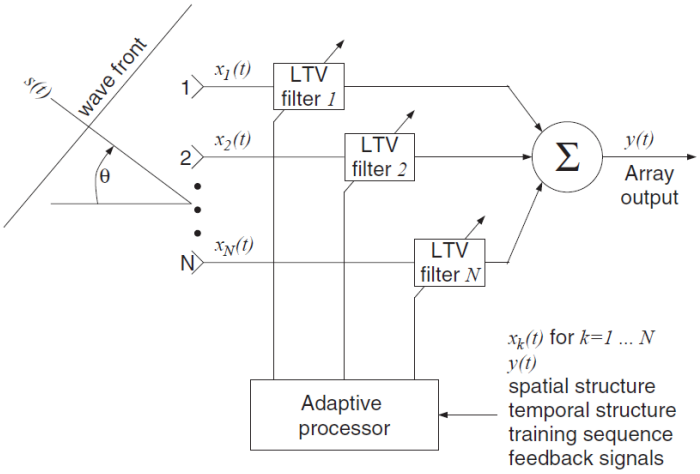

Figure 5: Functional diagram of an *N* element Adaptive antenna [3].

3.1 Receiver

Figure 6a shows schematically the block diagram of the receiver part of the adaptive antenna system. In addition to the antenna itself, it contains a radio unit, a beam forming unit, and a signal processing unit.

The number of elements in the array should be relatively low (up to 8 for LTE-Advanced), in order to avoid unnecessarily high complexity in the signal processing unit. Array antennas can be one-, two-, and three-dimensional, depending on the dimension of space one wants to access.

The radio unit consists of down-conversion chains and (complex) analog-to-digital conversion (A/D). There must be *M* down-conversion chains, one for each of the array elements. The received signals from the mobile units are combined into one, which is the input to the remaining part of the receiver (amplifier, channel decoding, etc.).

Based on the received signal, the signal-processing unit calculates the complex weights $w_1, w_2, \ldots, w_M$ with which the received signal from each of the array elements is multiplied. These weights will determine the antenna pattern in the uplink direction. The estimate of the weights can be optimized using one of the two main criteria depending on the application and complexity:

a. Maximization of the power of the received signal from the desired user or
b. Maximization of the SIR by suppressing the signal received from the interference sources (adaptive array).

In theory, with M antenna elements M − 1 sources of interference can be "nulled out", but this number will normally be lower due to the multipath propagation environment.

3.2 Transmitter

The transmitter part of the adaptive antenna is illustrated in Figure 6b. The signal is split into *M* branches, which are weighted by the complex weights $w_1, \ldots, w_M$ in the beam forming unit. The weights determine the radiation pattern in the downlink direction, are calculated as before by the signal processing unit. The radio unit consists of D/A converters and the up converter chains.

The principal difference between uplink and downlink is that no knowledge of the spatial channel response is available on downlink. In a time division duplex (TDD) system the mobile station and base station use the same carrier frequency only separated in time. In this case the weights calculated on uplink will be optimal on downlink if the channel does not change during the period from uplink to downlink transmission. However, this cannot be assumed to be the case in general, at least not in systems where the users are expected to move at high speed. If frequency division duplex (FDD) is used, the uplink and downlink are separated in frequency. In this case the optimal weights will generally not be the same because of the channel response dependency on frequency.

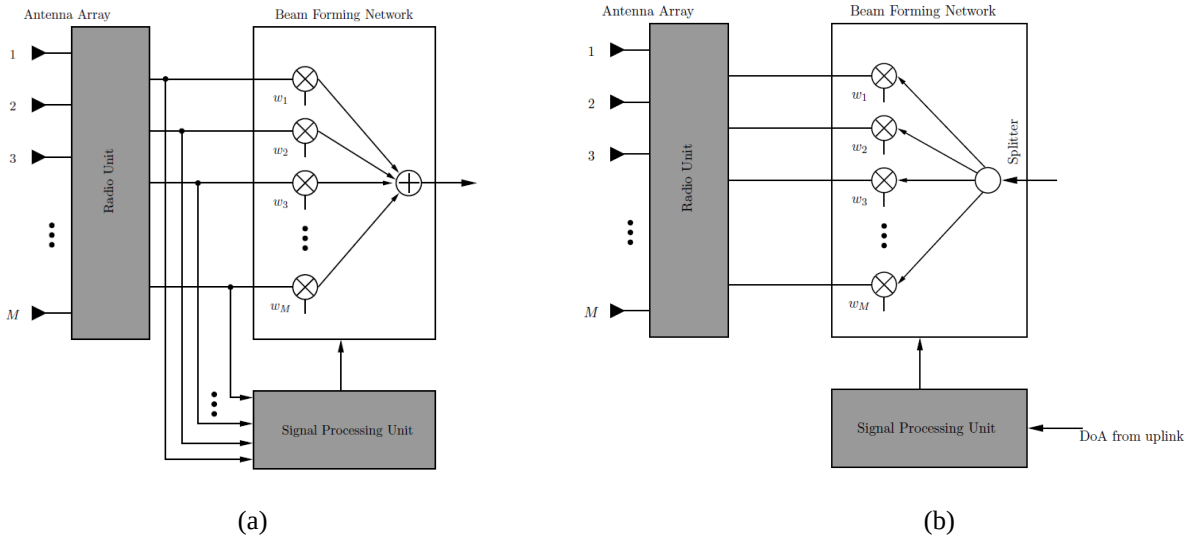

Figure 6: Receiver (a) and transmitter (b) part of an adaptive antenna [3].

4. Overview of Direction-Of-Arrival (DOA) Algorithms

The DOA algorithm determines the directions of all incoming signals based on the time delays [4]. Consider an M × N planar array with inter-element spacing d_x along the x-axis and d_y along the y-axis as shown in Figure 7. When an incoming signal *s(t)* impinges at an angle (θ, φ) on the antenna array, it produces time delays relative to the other antenna elements. For the rectangular array in Figure 7, the time delay of the signal *s(t)* at the (m, n)th element, relative to the reference element (0, 0) at the origin, is

$$\tau_{mn} = \frac{\Delta r}{c_0} \tag{1}$$

where $\Delta r = d_{mn}\cos(\psi)$ and c_0 represent respectively the differential distance and the speed of the light in free-space. The differential distance, Δr, is computed using

$$\Delta r = d_{mn}\cos(\psi) \tag{2}$$

where d_{mn} is the distance between the origin and the (m, n)th element, and ψ is the angle between the radial unit vector from the origin to the (m, n)th element and the radial unit vector in the direction of the incoming signal $s(t)$. Subsequently, d_{mn} and $\cos(\psi)$ are determined using

$$d_{\text{mn}} = \sqrt{m^2 d_x^2 + m^2 d_x^2} \tag{3}$$

$$\cos(\psi) = \frac{\hat{\boldsymbol{a}}_{\boldsymbol{r}} \cdot \hat{\boldsymbol{a}}_{\boldsymbol{\rho}}}{|\hat{\boldsymbol{a}}_{\boldsymbol{r}}||\hat{\boldsymbol{a}}_{\boldsymbol{\rho}}|} \tag{4}$$

where $\hat{\boldsymbol{a}}_{\boldsymbol{r}}$ and $\hat{\boldsymbol{a}}_{\boldsymbol{\rho}}$ are, respectively, the unit vectors along the direction of the incoming signal s(t) and along the distance d_{mn} to the (m, n)th element.

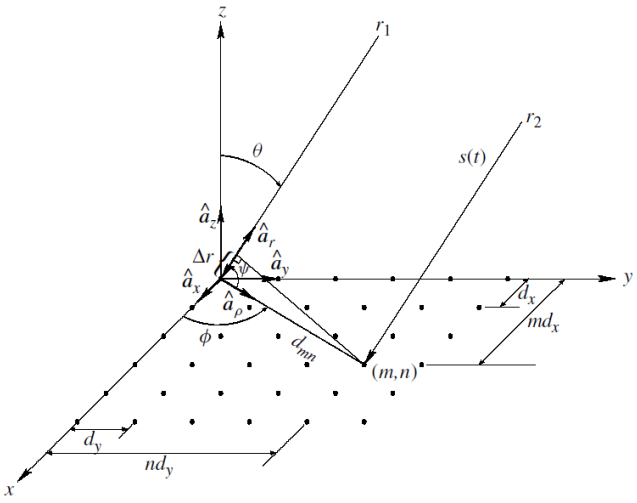

Figure 7: M × N planar array with graphical representation of the time delay.

DOA estimation techniques can be categorized on the basis of the data analysis and implementation into four different areas: conventional methods, subspace-based methods, and maximum likelihood methods [5].

Conventional methods for DOA estimation are based on the concepts of beamforming and null steering and do not exploit the statistics of the received signal. The DOA of all the signals is determined from the peaks of the output power spectrum obtained from steering the beam in all possible directions. Examples of conventional methods are the delay-and-sum method (classical beamformer method or Fourier

method) and Capon's minimum variance method. One major disadvantage of the delay-and-sum method is its poor resolution; that is, the width of the main beam and the height of the sidelobes limit its ability to separate closely spaced signals [5]. Capon's minimum variance technique tries to overcome the poor resolution problem associated with the delay-and-sum method and gives a significant improvement, but it fails when the SNOIs are correlated with the SOI.

Subspace methods exploit the structure of the received data, resulting in a dramatic improvement in resolution. Two examples are the MUltiple SIgnal Classification (MUSIC) algorithm [6] and the Estimation of Signal Parameters via Rotational Invariance Technique (ESPRIT). The MUSIC algorithm provides information about the number of incident signals, DOA of each signal, strengths and cross correlations between incident signals, and noise powers. However it is computationally intensive, and requires very precise and accurate array calibration. It also fails if the impinging signals are highly correlated because the covariance matrix of the received signals becomes singular.

The ESPRIT algorithm is another subspace-based DOA estimation technique and has several advantages over MUSIC, such as that it

1. is less computationally intensive,
2. requires much less storage,
3. does not involve an exhaustive search through all possible steering vectors to estimate the DOA, and
4. does not require the calibration of the array.

Maximum Likelihood (ML) techniques are less popular than the subspace techniques because ML methods are computationally intensive. However, ML techniques outperform the subspace-based techniques in low SNR and in correlated signal environment [7].

5. ARRAY WEIGHTS AND THE WEIGHTED RESPONSE

Figure 8 below is an illustration of the beamforming concept [8]. The signal x_n from each element is multiplied by a complex conjugated weight w_n^*. The weighted signals are added together to form the output signal. The output signal y is therefore given by

$$y = \sum_{n=1}^{M} w_n^* x_n = \mathbf{w}^H \mathbf{x} \tag{5}$$

where **w** represents the length M vector of weights, **x** represents the length M vector of received signals and the superscript H represents the conjugate transpose of a vector.

The signal received is summed over the signals from multiple users, one of which is designated as the "desired" signal. The weights are adjusted according to the received data, either to enhance the data signal or cancel out the interferences. The received data will be a sum of signal, interference and additive white Gaussian noise (AWGN) such that

$$\mathbf{x} = \alpha \mathbf{h}_0 + \mathbf{n} \tag{6}$$

$$\mathbf{n} = \sum_{n=1}^{N} \alpha_n \mathbf{h}_n + \text{noise} \tag{7}$$

The goal of beamforming or interference cancellation is to isolate the signal of the desired user, contained in the term α, from the interference and noise. The vectors $\mathbf{h}_n$ are the spatial signatures of the n^{th} user. In perfect line-of-sight conditions, this vector is the steering vector. However, in more realistic setting, this vector is a single realization of a random fading process. The model above is valid if we assume the fading is slow and flat such that it is constant over the symbol period or several symbol periods.

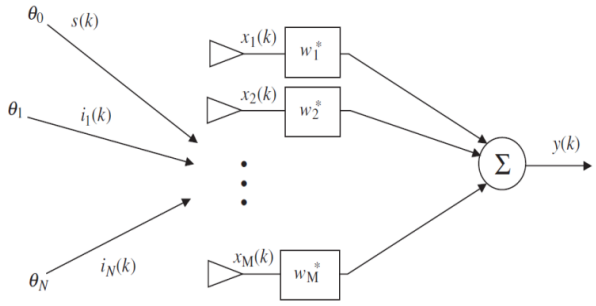

Figure 8: A general beamforming system.

6. BEAMFORMING ALGORITHMS

For optimal beamforming, a weighted vector that minimizes a cost function is determined. When the cost function is minimized, the quality of the signal is maximized at the array output [4]. Some commonly used optimal beamforming techniques include the Minimum Mean Square Error (MMSE), Maximum Signal-to-Noise Ratio (MSNR), and Minimum (noise) Variance (MV).

6.1 Minimum Mean Square Error (MMSE) Algorithm

The minimum mean squared error (MMSE) algorithm minimizes the error with respect to a reference signal d_k [8]. In this model, the desired user is assumed to transmit this reference signal, i.e., $\alpha = \beta d_k$, where β is the signal amplitude and d_k is known to the receiving base station. The output y_k is required to track this reference signal. The MMSE finds the weights w that minimize the average power in the error signal ε_k, the difference between the reference signal d_k and the output signal y_k obtained as

$$\varepsilon_k = d_k - \mathbf{w}^H \mathbf{x}_k \tag{8}$$

Thus, the MSE based cost function can be written as

$$J_{MSE}(\mathrm{E}[\varepsilon_k^2]) = \mathrm{E}[(d_k - \mathbf{w}^H \mathbf{x}_k)^2]$$

$$= \mathrm{E}[d_k^2 - 2d_k \mathbf{w}^H \mathbf{x}^k + \mathbf{w}^H \mathbf{x}_k \mathbf{x}_k^H \mathbf{w}] \quad (9)$$

$$= d_k^2 - 2\mathbf{w}^H \mathrm{E}[d_k \mathbf{x}_k] + \mathbf{w}^H \mathrm{E}[\mathbf{x}_k \mathbf{x}_k^H]\mathbf{w}$$

$$= d_k^2 - 2\mathbf{w}^H \mathbf{r}_{xd} + \mathbf{w}^H \mathbf{R}_{xx}\mathbf{w}$$

To find the minimum of this functional, we take its derivative with respect to the weights such that

$$\min_{\mathbf{w}}\{J_{MSE}(\mathrm{E}[\varepsilon_k^2])\} \Rightarrow \frac{\partial}{\partial \mathbf{w}}\{J_{MSE}(\mathrm{E}[\varepsilon_k^2])\} = 0 \quad (10)$$

Taking the derivative in (10) and solving in terms of the weights, **w**, yields the optimal antenna weight vector, such that

$$\mathbf{w}_{\text{opt}} = \mathbf{R}_{xx}^{-1} \mathbf{r}_{xd} \quad (11)$$

This solution is also known as the Wiener filter.

The MMSE technique minimizes the error with respect to a reference signal. This technique does not require knowledge of the spatial signature $\mathbf{h}_0$, but does require knowledge of the transmitted signal. This is an example of a training based scheme: the reference signal acts to train the beamformer weights.

6.2 Least Mean Square (LMS) Algorithm

The least mean square or LMS algorithm is another commonly used adaptive algorithm [4]. It updates the antenna weights at each iteration by estimating the gradient of the quadratic surface and then moving the weights in the negative direction of the gradient by a constant known as "step" [9]. It is a low complexity algorithm that does not require direct matrix inversion or memory. At each iteration of the adaptive process, the estimate of the gradient is of the form

$$\widehat{\nabla}[J(\mathbf{w})]_k = \begin{bmatrix} \frac{\partial J(\mathbf{w})}{\partial w_0} \\ \vdots \\ \frac{\partial J(\mathbf{w})}{\partial w_L} \end{bmatrix} \quad (12)$$

where $J(\mathbf{w})$ is the cost function to be minimized. Thus, according to the method of steepest descent, the iterative equation that updates the weights at each iteration is

$$\mathbf{w}_{k+1} = \mathbf{w}_k - \mu\widehat{\nabla}[J(\mathbf{w})]_k \quad (13)$$

where μ is the step size related to the rate of convergence. The LMS algorithm computes the weights iteratively as

$$\mathbf{w}_{k+1} = \mathbf{w}_k + 2\mu\mathbf{x}_k(d_k - \mathbf{x}_k^T\mathbf{w}_k) \quad (14)$$

To ensure the convergence of the weights, $\mathbf{w}_k$, the step size μ has to be bounded by the condition

$$0 < \mu < \frac{1}{\lambda_{\max}} \tag{15}$$

where λ_{max} is the maximum eigenvalue of the covariance matrix, $\mathbf{R}_{xx}$. The main disadvantage of the LMS algorithm is that it tends to converge slowly, especially in noisy environments.

7. BENEFITS OF SMART ANTENNA SYSTEMS

Benefits associated with smart antennas are manifold. These include increase in coverage range and capacity, smart handover, better quality of service, information security and access to user location.

7.1 Coverage Extension

Smart antennas can increase the range of coverage by a base station since they are able to focus their energy toward the intended users instead of directing and wasting it in other unnecessary directions. They are more directive than traditional sectorized or omnidirectional antennas and base stations can be placed further apart, potentially reducing the cluster re-use size and leading to more cost-efficient deployment [1]. Smart antenna systems are well-suited in rural and sparsely populated areas, where radio coverage rather than capacity is more important [5]. Moreover, using transmit and receive beams that are directed toward the mobile user of interest, the multipath [10] and the inter-symbol-interference, due to multipath propagation present in mobile radio environments are mitigated.

7.2 Capacity Improvement

In densely populated areas the main source of interference is from the other users. The deployment of adaptive arrays is to simultaneously increase the useful received signal level and lower the interference level, thus providing significant improvement in the Signal to Interference Ratio (SIR). An immediate impact to the increase of the SIR is the possibility for reduced frequency reuse distance. This will lead to a large capacity increase since more carriers can be allocated per cell.

a. FDMA–TDMA System with Switched Beams

Following the analysis in [11], the overall outage probability for the scenario with one tier of interfering cells can be calculated as

$$\mathrm{P}(s_w \leq p_R s_I, N_B) = \sum_{CCI} P(s_w \leq P_R s_I \mid cci) \cdot (6 - cci) \left(\frac{LF}{N_B}\right)^{cci} \left(1 - \frac{LF}{N_B}\right)^{6-cci} \tag{16}$$

where N_B is the number of beams, LF is the loading factor, s_w is the wanted signal, s_I is the interfering signal, p_r is some protection ratio, and $\mathrm{P}(s_w \leq p_R s_I \mid cci)$ is the conditional outage probability, that is, the

probability of co-channel interference (CCI) given that there are cci active interfering cells, and the omnidirectional case is given for $N_B = 1$.

In [11] it was shown that the ratio of the achieved spectral efficiencies with/without smart antennas is inversely proportional to the achieved cluster sizes. Based on the above, the cluster size can be calculated for given shadow fading and loading conditions for an outage criterion. The example plot shown in Figure 9 considers 6-dB shadow fading, 100% loading, and 1% outage. The values of 8 and 20 dB were used for the protection ratio, in order to cover a variety of modulation schemes.

The result in Figure 9 shows that the introduction of an adaptive multibeam antenna capable of forming 24 beams (8 beams per sector, as in Figure 2) will result in an eight- to tenfold increase in the spectral efficiency depending on modulation used.

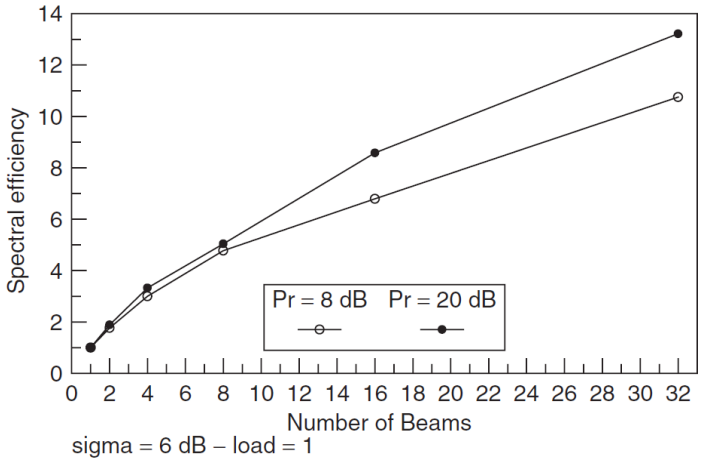

Figure 9: Spectral efficiency with an adaptive multibeam antenna.

b. Macrocells with CDMA

In [12] and [13], a method based on the radiation pattern characteristics was analyzed. The idea was based on the fact that the characteristics of the produced adaptive antenna pattern response (and, as a consequence, the performance of the system) are affected from parameters such as scattering of the environment, mutual coupling of the array elements, and other mismatches. If these effects are ignored, the estimated performance will be overly optimistic.

In [12] and [13], the BER probability was calculated from the equation

$$P_b = Q\left(\sqrt{3 \bullet SF \bullet SIR_{omni} \bullet G_{AA}}\right) \tag{17}$$

where SF is the spreading factor, SIR_{omni} is the signal-to-interference ratio with an omnidirectional antenna, and G_{AA} is the gain with adaptive antennas, calculated using the approximate interference

model for uniform distribution of users and a radiation pattern that is approximated as a stepped function with the ideal beamwidth and average sidelobe level:

$$G_{AA} = \begin{cases} \frac{1}{k}, & central\ cell \\ \frac{1}{k}\frac{5D}{3D+2}, & all\ cells \end{cases} \tag{18}$$

where "central cell" and "all cells" refer to how many base stations employ smart antennas (four tiers are assumed for the latter scenario), D is the directivity of the radiation pattern, and

$$k = \frac{BW}{2\pi} + SLL\left(1 - \frac{BW}{2\pi}\right) \tag{19}$$

with BW and SLL the ideal or effective beamwidth and sidelobe level, respectively.

Figure 10 shows a plot of the SIR gain as a function of the achieved beamwidth and average sidelobe level, when the smart antenna is deployed only at the central cell. When the effective beamwidth is 10° to 40° and the effective average sidelobe level is −10 to −20 dB, the results show that spatial filtering can offer gains between 7 and 14 dB.

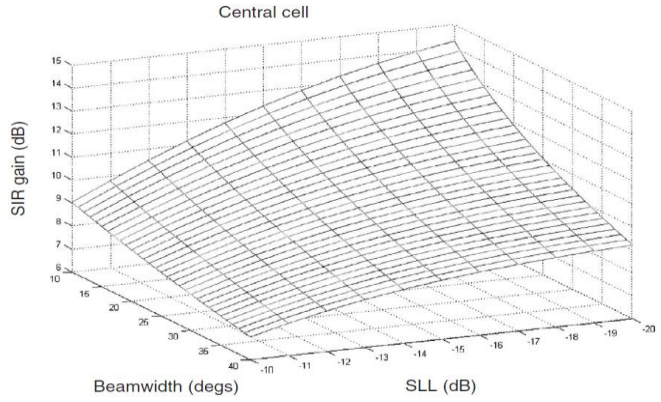

Figure 10: SIR gain as a function of beamwidth and sidelobe level.

7.3 Smart Handover and Efficient Power Control

Smart antenna provides diversity gain to reduce fading of the radio signal, thus better power control can be achieved. Furthermore, if user location information is combined with the handover mechanism, "soft/softer" and "hard" handovers can now become "smart handovers."

Spatial filtering of smart antennas can also provide the necessary RF power balancing between the different cells [14], if handover between cells of different layers in a hierarchical cell structure needs to be supported on the same carrier to increase spectral efficiency. However, more complex radio resource management is needed to handle near-far situations between the different cell layers.

7.4 Better Quality of Service (QoS)

In noise or interference limited environments, the gain achieved by an antenna array can enhance signal quality (i.e., lower BER). This is demonstrated in Figures 11 and 12. Figure 11.37 considers the probability of detection (PD) for the case when a matched filter is employed for each antenna array element. From [15],

$$P_D = Q(Q^{-1}(P_F) - \sqrt{M \cdot SNR}) \tag{20}$$

where $Q(\cdot)$ is the Q function, P_F is the threshold probability of false alarm, M is the number of antenna elements, and SNR is the signal-to-noise ratio.

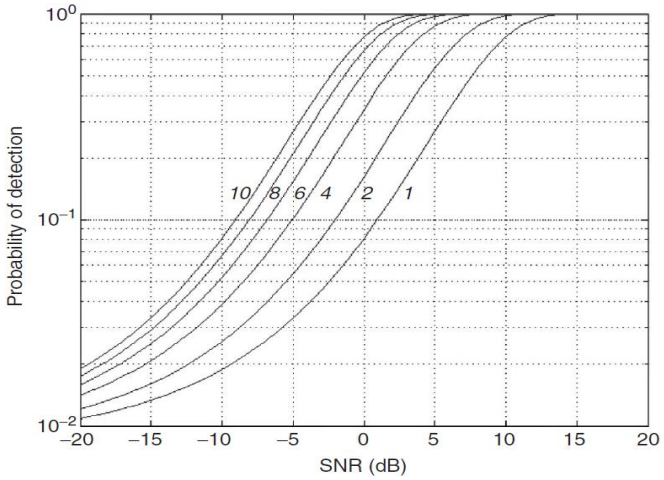

Figure 11: Probability of detection for matched filtering with different antenna array elements.

Figure 11 shows the detection performance (and hence QoS) can be significantly enhanced with an antenna array. For example, with 0-dB SNR there is 8% probability of detection with a single element, 16% with two elements, 34% with four, 52% with six, 66% with eight, and 77% with ten.

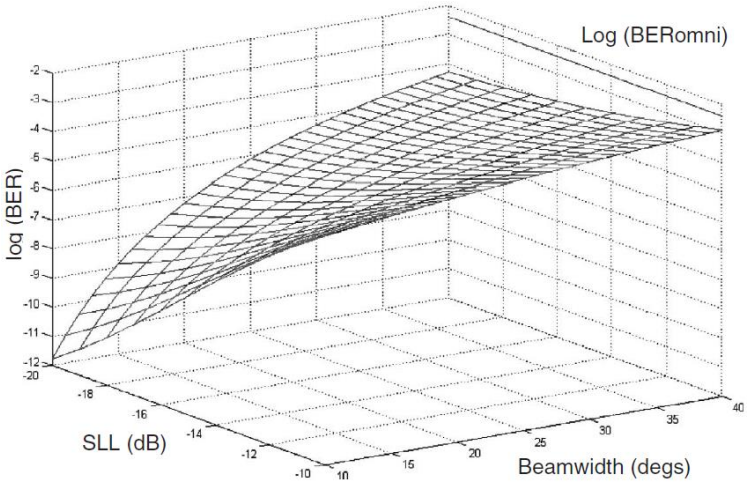

Figure 12: BER versus beamwidth and sidelobe level.

Figure 12 shows results of achieved BER versus beamwidth and sidelobe level produced by the smart antenna in a large cell with DS-CDMA. Considerable BER gain is achieved for beamwidth between 10° and 40°, and sidelobe levels between −10 and −20 dB. If the smart antenna can achieve 30° beamwidth, then an improvement of 1 to 3 orders of magnitude for the BER can be accomplished with average sidelobe levels between −10 and −20 dB.

7.5 Improved Information Security

In a society that becomes more dependent on conducting business and distributing personal information, security is an important issue. Smart antennas make it more difficult to tap a connection because the intruder must be positioned in the same direction as the user as "seen" from the base station to successfully tap a connection [5].

7.6 Accurate Access to User Location

Due to the spatial detection nature of smart antenna systems, the network will have access to spatial information about users [1]. This information may be exploited in estimating the positions of the users much more accurately than in existing networks. Consequently, exact positioning can be used in services to locate humans in case of emergency calls or for any other location-specific service.

8. DRAWBACKS OF SMART ANTENNA SYSTEMS

While smart antennas provide many benefits, they do suffer from certain drawbacks. For example, their transceivers are much more complex than traditional base station transceivers. The antenna needs separate transceiver chains for each array antenna element and accurate real-time calibration for each of them [5]. Moreover, the antenna beamforming is computationally intensive, which means that smart-antenna base stations must be equipped with very powerful digital signal processors. This tends to increase the system costs in the short term, but since the benefits outweigh the costs, it will be less expensive in the long run. For a smart antenna to have pattern-adaptive capabilities and reasonable gain, an array of antenna elements is necessary.

9. SIMULATION AND ANALYSIS

A MATLAB program based on the LMS algorithm is written to perform beamforming with a linear array of M isotropic antenna elements.

9.1 Classical Phased Array versus Adaptive Array

To compare the beamforming effects between a classical phased array which only uses equal amplitude excitations and an adaptive array, let us consider the following example. For an eight-element linear array of isotropic elements with spacing d = 0.5λ, there are two incoming signals: a pilot signal (SOI) incident from $\theta_0 = 20^\circ$, and an interfering signal (SNOI) incident from $\theta_1 = 45^\circ$. The radiation characteristics for both the classical and the adaptive arrays are plotted from Figure 13 to 16. The results are also summarized in Table 1.

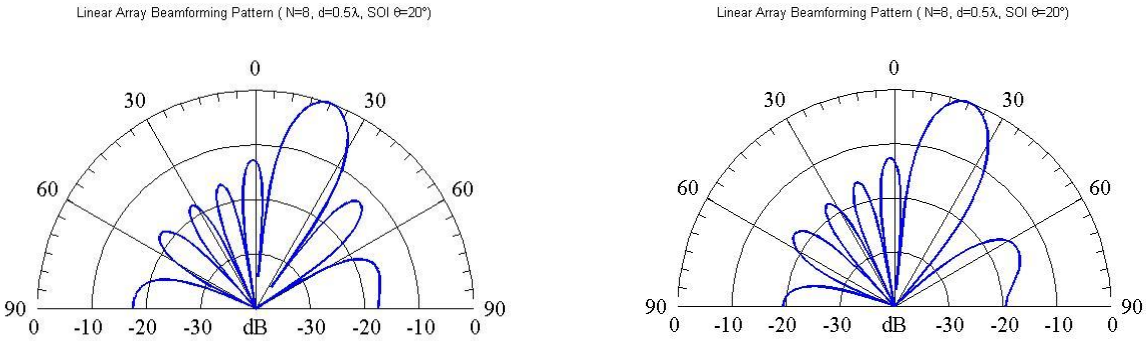

(a) (b)

Figure 13: Normalized patterns of eight-element (a) classical phased array and (b) adaptive array using LMS in polar coordinates.

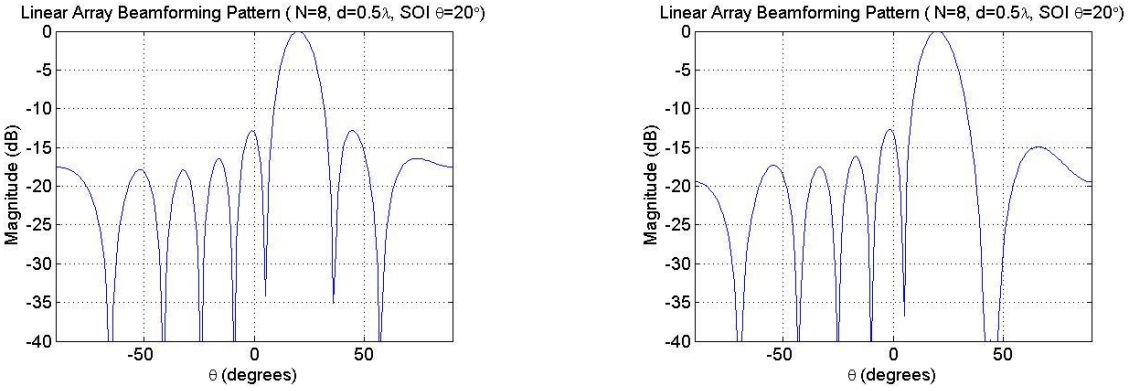

(a) (b)

Figure 14: Normalized patterns of eight-element (a) classical phased array and (b) adaptive array using LMS in rectangular coordinates.

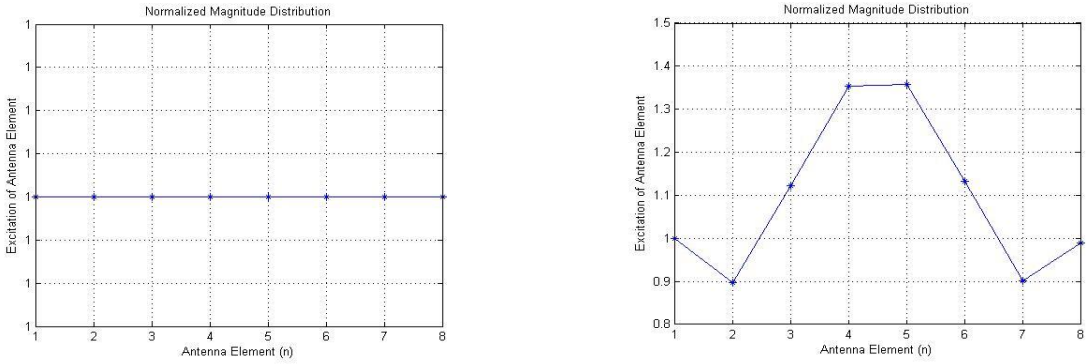

(a) (b)

Figure 15: Normalized magnitude distributions of eight-element (a) classical phased array and (b) adaptive array using LMS.

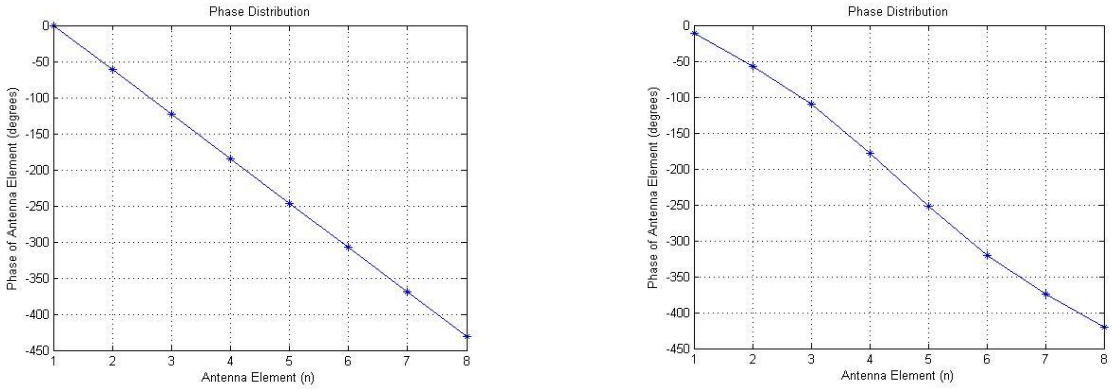

(a) (b)

Figure 16: Phase distributions of eight-element (a) classical phased array and (b) adaptive array using LMS.

Table 1: Amplitude (w's) and phase (β's) excitation coefficients of 8-element classical phased array and adaptive array using LMS algorithm (d = 0.5λ, SOI = 20˚, SNOI = 45˚, μ = 0.01, 81 iterations).

	Element	**1**	**2**	**3**	**4**	**5**	**6**	**7**	**8**
Classical	*w*	1	1	1	1	1	1	1	1
Array	*β*	0	−61.56	−123.12	−184.69	−246.25	−307.82	−369.38	−430.95
Adaptive	*w*	1	0.8982	1.1384	1.3760	1.3760	1.1384	0.8982	1
Array	*β*	−11.62	−57.05	−109.98	−178.77	−252.21	−321.01	−373.94	−419.37

Both arrays have main lobe directed at the SOI of $\theta_0 = 20^\circ$. The classical phased array uses uniform element excitations with linear progressive phase shifts. It has formed seven nulls, but it does not place the null toward the SNOI at $\theta_1 = 45^\circ$, so it does not have the noise cancellation capability in general. While the adaptive array has formed six nulls and placed one of the nulls at $\theta_1 = 45^\circ$, it is evident that the obtained pattern has the capability of cancelling out the interfering signal. It is also observed that the amplitude excitation coefficients of the adaptive array are symmetrical about the center of the array (4–5th element). The element excitation coefficients and phase shifts are no longer uniform and linear.

9.2 Four-Element Adaptive Array with One versus Two SNOI's

All the setups are the same as previous example, except now we use a four-element array and have two cases. For case one, there is only one SNOI at $\theta_1 = 45^\circ$, which is the same as before; and for case two, there is one more SNOI at $\theta_2 = 70^\circ$. The radiation characteristics for both cases are plotted from Figure 17 to 20.

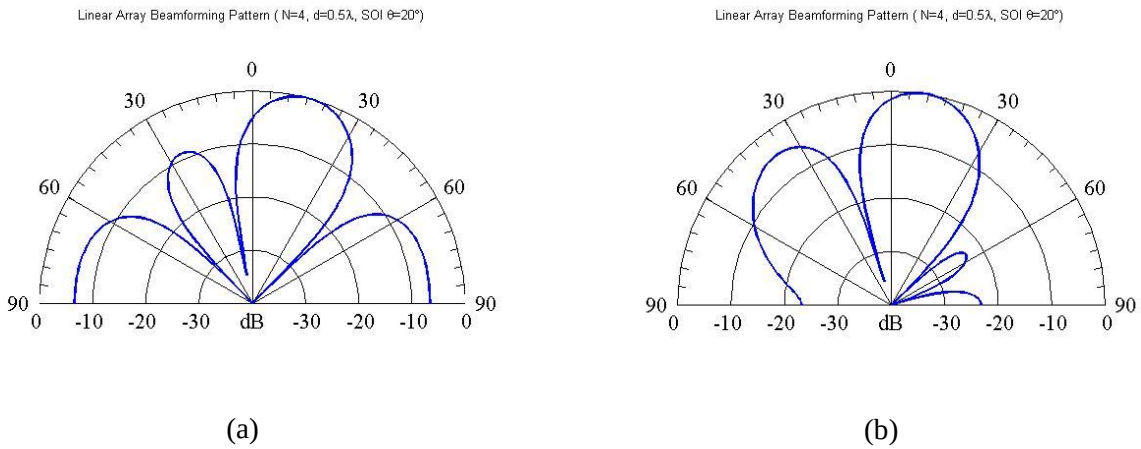

(a) (b)

Figure 17: Normalized patterns of four-element adaptive array with (a) only one SNOI versus (b) two SNOI's using LMS in polar coordinates.

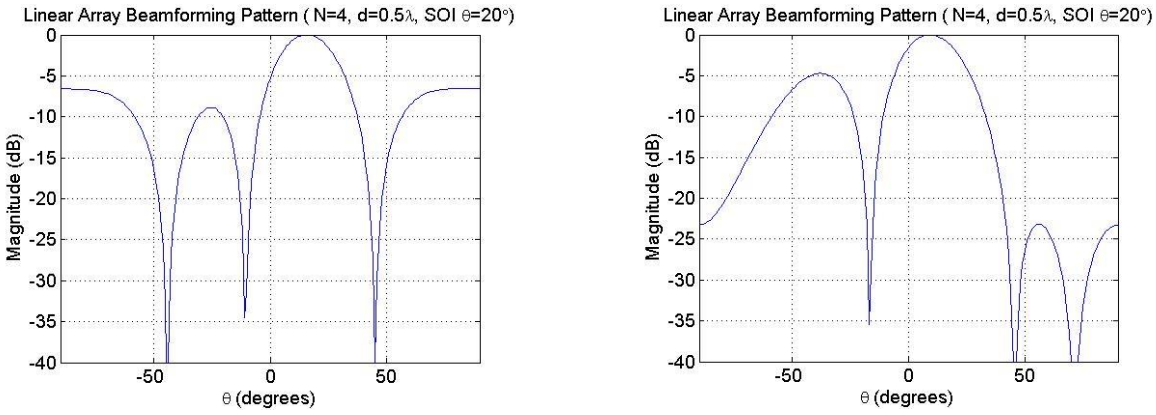

(a) (b)

Figure 18: Normalized patterns of four-element adaptive array with (a) only one SNOI versus (b) two SNOI's using LMS in rectangular coordinates.

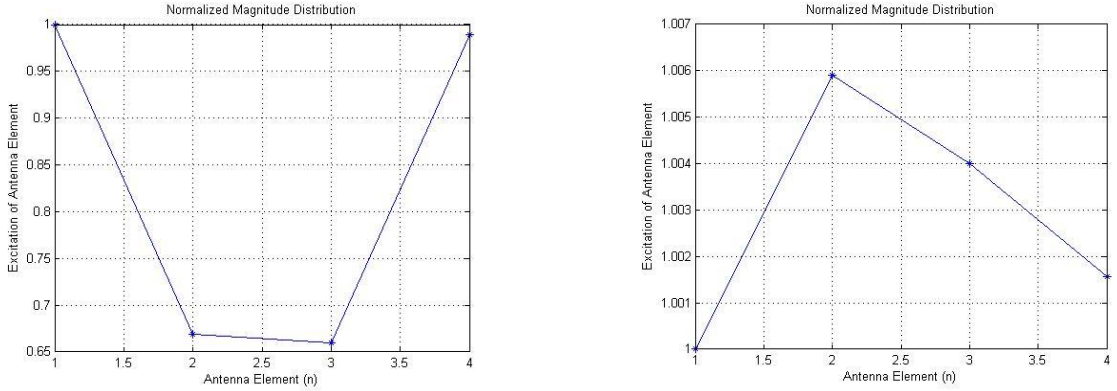

(a) (b)

Figure 19: Normalized magnitude distributions of four-element adaptive array with (a) only one SNOI versus (b) two SNOI's using LMS.

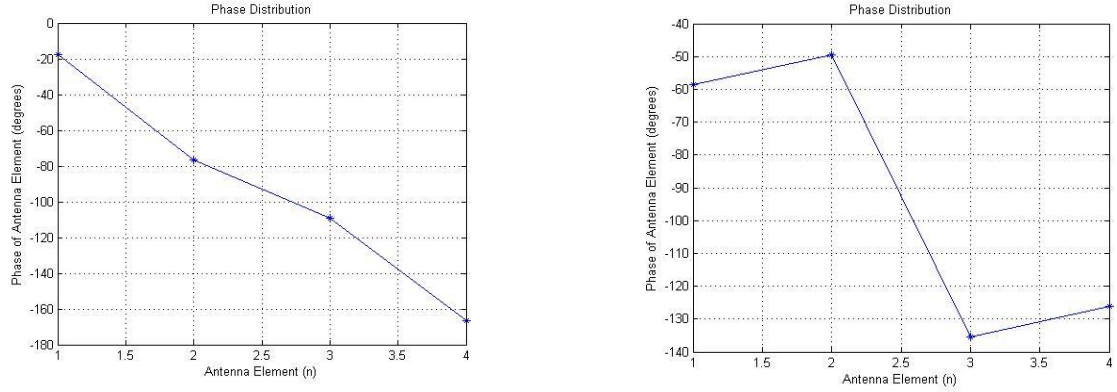

(a) (b)

Figure 20: Phase distributions of four-element adaptive array with (a) only one SNOI versus (b) two SNOI's using LMS.

With only one SNOI, the main lobe of the array is directed at the SOI of $\theta_0 = 20^\circ$, while with one more SNOI added, the main lobe direction is slightly off $\theta_0 = 20^\circ$. Comparing with the previous example with eight-element array, the four-element array has broader main lobe and higher side lobes, which can result in weaker resolution of the SOI. However, both cases have demonstrated good capability of cancelling out SNOI's. With one SNOI, the array has placed a null at $\theta_1 = 45^\circ$, and with two SNOI's, the array has placed an additional null at $\theta_2 = 70^\circ$ very accurately. Both cases have formed three nulls. In general, an adaptive array can cancel out up to M−1 SNOI's if the SNOI's have large enough angular separations, where M is the total number of array elements.

10. SUMMARY AND CONCLUSIONS

This report has provided a general overview of the smart antenna system. Smart antennas are the antennas with intelligence and the radiation pattern can be adaptively changed without using any mechanical means. They utilize SDMA, adds another resource dimension to the existing TDMA, FDMA and CDMA systems. With appropriate adaptive algorithms such as Least Mean Square (LMS) Algorithm the beam forming can be obtained. As the system uses a DSP processor the signals can be processed digitally and the performance with a high data rate transmission and good reduction of mutual signal interference. Comparing with some existing systems, they can provide better coverage range and capacity, smart handover, better quality of service, information security and access to user location. Ultimately, smart antennas can further improve network efficiencies of the next generation mobile communication network.

REFERENCES

1. I. Stevanovi´c, A. Skrivervik, and J. R. Mosig, "Smart antenna systems for mobile communications," Ecole Polytechnique F ´ed ´erale de Lausanne, Lausanne, Suisse, Tech. Rep., Jan. 2003. [Online]. Available: http://lemawww.epfl.ch

2. C. A. Balanis, "Modern Antenna Handbook", Chapter 11, Wiley-Interscience; 1 edition (August 2008)

3. C. A. Balanis, P. I. Ioannides, "Introduction to Smart Antennas – Synthesis Lectures on Antenna", Morgan & Claypool Publishers; 1 edition (June 15 2007)

4. C.A.Balanis, "Antenna Theory and Design", Chapter 8, Wiley, New York; 1997, 2nd ed.

5. J. C. Liberti, Jr., and T. S. Rappaport, "Smart Antennas for Wireless Communications: IS-95 and Third Generation CDMA Applications", Prentice Hall PTR, Upper Saddle River, NJ, 1999.

6. R. O. Schmidt, "Multiple Emitter Location and Signal Parameter Estimation," Proceedings of RADC Spectrum Estimation Workshop, Griffiss AFB, New York, pp. 243–258, 1979.

7. I. Ziskind and M. Wax, "Maximum Likelihood Localization of Multiple Sources by Alternating Projection," IEEE Trans. Acoustics, Speech, and Signal Process., Vol. 36, No. 10, pp.1553–1560, Oct. 1988.

8. R.S.Adve, "Direction of Arrival Estimation", course notes, [Online]. Available: http://www.comm.utoronto.ca/~rsadve/Notes/DOA.pd

9. S. Haykin, "Adaptive Filter Theory", Prentice Hall, Englewood Cliffs NJ, 2002.

10. L. C. Godara, "Applications of antenna arrays to mobile communications. Part II: Beamforming and direction-of-arrival considerations," in Proc. IEEE, vol. 85, Aug. 1997, pp. 1195–1245.

11. S. C. Swales, M. A. Beach, D. J. Edwards, and J. P. McGeehan, "The performance enhancement of multibeam adaptive base-station antennas for cellular land mobile radio systems", IEEE Trans. Vehicular Technol., Vol. 39, No. 1, pp. 56–67, February 1990.

12. G. V. Tsoulos, "On the single and multiple cell deployment of adaptive antennas with CDMA", IEE Electron. Lett., Vol. 34, No. 23, pp. 2196–2197, November 12, 1998.

13. G. V. Tsoulos, “Approximate SIR and BER formulas for DS-CDMA based on the produced radiation pattern characteristics with adaptive antennas”, IEE Electron. Lett., Vol. 34, No. 19, pp. 1802–1804, September 17, 1998.

14. G. V. Tsoulos, G. E. Athanasiadou, M. A. Beach, and S. C. Swales, “Adaptive antennas for microcellular and mixed cell environments with DS-CDMA”, Wireless Personal Commun. J., Special Issue on CDMA for Universal Personal Communications Systems, Vol. 7, No. 2/3, pp. 147–169, August 1998.

15. D. Johnson and D. Dudgeon, Array Signal Processing, Prentice Hall, Englewood Cliffs, NJ, 1993.